environments

MDPI

Review

Critical Review of Life Cycle Assessment of Hydrogen Production Pathways

Manfredi Picciotto Maniscalco [1,*], Sonia Longo [2], Maurizio Cellura [2], Gabriele Micciché [2,3] and Marco Ferraro [1]

[1] Consiglio Nazionale delle Ricerche, Istituto di Tecnologie Avanzate per l'Energia "Nicola Giordano", Viale delle Scienze Edificio 9, 90128 Palermo, Italy; marco.ferraro@itae.cnr.it
[2] Department of Engineering, University of Palermo, Viale delle Scienze Edificio 9, 90128 Palermo, Italy; sonia.longo@unipa.it (S.L.); maurizio.cellura@unipa.it (M.C.); gabriele.micciche@unipa.it (G.M.)
[3] Centre for Sustainability and Ecological Transition, University of Palermo, Piazza Marina 61, 90133 Palermo, Italy
* Correspondence: maniscalco@itae.cnr.it

Abstract: In light of growing concerns regarding greenhouse gas emissions and the increasingly severe impacts of climate change, the global situation demands immediate action to transition towards sustainable energy solutions. In this sense, hydrogen could play a fundamental role in the energy transition, offering a potential clean and versatile energy carrier. This paper reviews the recent results of Life Cycle Assessment studies of different hydrogen production pathways, which are trying to define the routes that can guarantee the least environmental burdens. Steam methane reforming was considered as the benchmark for Global Warming Potential, with an average emission of 11 kg_{CO2eq}/kg_{H2}. Hydrogen produced from water electrolysis powered by renewable energy (green H_2) or nuclear energy (pink H_2) showed the average lowest impacts, with mean values of 2.02 kg_{CO2eq}/kg_{H2} and 0.41 kg_{CO2eq}/kg_{H2}, respectively. The use of grid electricity to power the electrolyzer (yellow H_2) raised the mean carbon footprint up to 17.2 kg_{CO2eq}/kg_{H2}, with a peak of 41.4 kg_{CO2eq}/kg_{H2} in the case of countries with low renewable energy production. Waste pyrolysis and/or gasification presented average emissions three times higher than steam methane reforming, while the recourse to residual biomass and biowaste significantly lowered greenhouse gas emissions. The acidification potential presents comparable results for all the technologies studied, except for biomass gasification which showed significantly higher and more scattered values. Regarding the abiotic depletion potential (mineral), the main issue is the lack of an established recycling strategy, especially for electrolysis technologies that hamper the inclusion of the End of Life stage in LCA computation. Whenever data were available, hotspots for each hydrogen production process were identified.

Keywords: hydrogen; LCA; electrolysis

Citation: Maniscalco, M.P.; Longo, S.; Cellura, M.; Micciché, G.; Ferraro, M. Critical Review of Life Cycle Assessment of Hydrogen Production Pathways. *Environments* **2024**, *11*, 108. https://doi.org/10.3390/environments11060108

Academic Editors: Tamíris Da Costa, Nick Holden, Daniele Costa and Mateus Guimarães da Silva

Received: 4 April 2024
Revised: 8 May 2024
Accepted: 16 May 2024
Published: 24 May 2024

1. Introduction

The use of fossil fuels stands as the predominant source of greenhouse gas emissions attributable to anthropogenic activities, accelerating global climate change and pressing for immediate and decisive measures to reduce GHG emissions [1]. The strategic implementation of hydrogen as an energy carrier, with its high energy content and potential to be produced from renewable resources, has emerged as a promising candidate to be part of the future global energy framework. In 2022, the global H_2 production of EU 27, EFTA and UK accounted for 11,333 kt, with more than 90% coming from reforming processes [2]. The 2023 Global Hydrogen Review, published by the International Energy Agency, indicated a substantial rise in global hydrogen consumption, particularly within the refining and chemical industries. However, this expansion has primarily been facilitated by increased production from fossil fuels, without yielding tangible benefits in terms of climate change mitigation [3]. The integration of hydrogen into novel sectors such as the hard-to-abate industry, transportation,

the synthesis of hydrogen-derived fuels, or electricity generation and storage—which are all crucial aspects for facilitating the transition to clean energy—remains marginal, constituting less than 0.1% of the global demand. According to the International Energy Agency's Net Zero Emissions for 2050 Scenario, hydrogen utilization is projected to increase by 6% annually until the conclusion of the current decade. Hence, there is an urgent call for defining low-emission routes for hydrogen production that could both satisfy the increasing demand and have a lower impact on the environment, especially with respect to climate change.

Different review papers have been published in the last decade [4–17], tackling the topic under different perspectives and in relation to different technologies. In [5–7,10–13,15–17], the authors focused the attention on specific conversion processes and inlet feedstock, with great efforts to define the best solutions, but limiting the comparison with all the other possible available technologies. The work conducted by Chelvam et al. [4] is centered mostly on the methodological aspects of the LCA conducted from 2002 to 2022, without the purpose of defining the eco-profile of the different processes. Bush et al. [8] conducted a systematic review of numerous production routes, but they referred to the results only in terms of the GWP. Wilkinson et al. [9] conducted an in-depth analysis of the methodological aspects of numerous LCAs, reporting the paramount results of the GWP for the main production processes and marking a trend of the other impact categories that refer to processes with GHG emissions lower than 3.6 kg_{CO2eq}/kg_{H2}. This latter parameter was set by the authors and expresses the value equal to 1.5 times the UK Low Carbon Hydrogen Standard.

Despite the relevant literature, the main purpose of this review is to provide a wide overview of the different hydrogen production technologies, analyzing results on different impact categories. This decision comes from the need of broadening the analysis beyond the only GWP since other critical aspects need to be tackled, as reported in the JRC workshop on fuel cells and H_2 production [18]. In fact, the use of renewable energy production systems can significantly impact the Acidification Potential (AP) and the Abiotic Depletion Potential (ADP). Similarly, the materials used in the electrolyzers raise the impacts on ADP due to the lack of available recycle strategies. Hence, these aspects together with Human Toxicity were included in the present work. Moreover, whenever information was available, the analysis was supported by hotspot identification for the system manufactory and use phase to identify processes and material that contribute the most to the environmental burdens. Finally, a statistical analysis of the results of each hydrogen production route was conducted to evaluate whether they converge or present a more scattered trend.

2. Context

Hydrogen is recognized for its potential as a sustainable energy carrier and can be produced through various processes. The 'hydrogen colour classification' system is an organized method to categorize these production techniques, based on the energy resources and processes employed. Although there is no unique definition for the color classification, and the European Parliament is moving away from this distinction [19], to ease the reading of this paper, the color classification proposed in [20] will be used. This distinction is also schematically presented in Figure 1. Arrows in the conversion process technologies represent the eventual by-products generated. The filled arrows represent solid by-products while the ones without the filling represent gaseous by-products. The conversion processes represented in the figure includes:

- Brown Hydrogen: produced via coal gasification, followed by syngas processes and gas purification.
- Grey and Blue Hydrogen: Derived from Steam Methane Reforming (SMR). The distinction between 'grey' and 'blue' lies in the CO_2 management; while grey results in direct CO_2 emissions, blue employs carbon capture techniques to mitigate the greenhouse gas release.
- Turquoise Hydrogen: Produced through Methane Pyrolysis. Methane pyrolysis involves the thermal decomposition of methane under oxygen-absent conditions, leading to the formation of hydrogen and solid carbon.

- Yellow Hydrogen: Obtained via grid-connected electrolysis. Electrolysis is the electrochemical process of water decomposition into hydrogen and oxygen using electrical energy.
- Green Hydrogen: generated from electrolysis powered exclusively by renewable energy sources.
- Pink hydrogen: refers to hydrogen produced via water electrolysis powered by a nuclear plant.

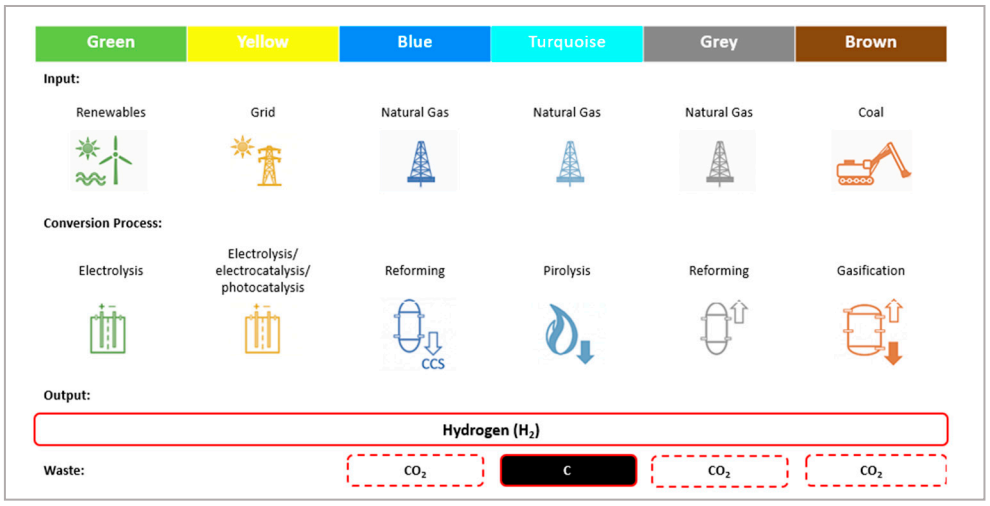

Figure 1. Hydrogen Production Pathways Overview.

In addition, in this review, the following other processes that are not included in hydrogen color classification were included:

- Copper–Chlorine (Cu-Cl) water splitting.
- Sulfur–Iodine (S-I) cycles.
- Plastic wastes pyrolysis and gasification.
- Waste biomass pyrolysis.
- Anaerobic digestion, hydrolysis and the fermentation of biological waste.

3. Life Cycle Assessment

This section presents the findings derived from Life Cycle Assessment (LCA) investigations pertaining to various hydrogen production methodologies documented in the scientific literature. The initial phase of data aggregation involved the systematic exploration of the Scopus database utilizing specific search queries: "LCA hydrogen production", "Life cycle assessment hydrogen production", "LCA H_2", and "LCA hydrogen". Out of the initial pool of papers found, the following screening criteria were used to identify the papers to be included in the review. Firstly, the panel was restricted to studies published during the last five years. Secondly, the skimming process was done to include titles related to hydrogen production processes and technologies and, thirdly, a screening of the abstract allowed us to consider only papers related to LCA or a specific environmental index. Finally, we excluded all the works already reported in other reviews, unless it was possible to include significant information previously omitted. So, a total of 21 papers were selected for extracting data.

The following section displays the results of the methodological and technical analysis of the collected papers. Regarding the methodological approach, distinctions and evaluations were done in relation to the publication year, data quality, LCI database, LCIA methods, LCA software, functional unit (FU), system boundaries, impact indicators and allocation methods. The technical analysis primarily concentrated on the impact indicator results, trying to identify the hotspots of the processes whenever data were available. Finally, a statistic analysis of the results is presented.

3.1. Methodological Insight

In a temporal prospective, out of the 21 papers analyzed, 4 were published in 2022, 12 in 2023 and 5 during the first month of 2024. Nine different functional units (FU) were found. Eight are related to the production of 1 kg of H_2 with different specifications of the final pressure, temperature and hydrogen purity grade, while only in one paper was 1 ton of H_2 found as FU. For this latter case, the results were scaled to 1 kg of H_2. Within the first category, one kilogram of hydrogen, without any further specification on the final stage conditions, was adopted in 11 studies. Two papers also specified a final purity grade equal or higher than 99.9%, while the major differences among the rest of the works are related to the final pressure of the produced hydrogen, which was accounted equal to: 25 bar (one paper), 30 bar (one paper), 925 psig (one paper), 80 bar (two papers) and 200 bar (two papers). To enhance comparability, Valente et al., [21] proposed a harmonization protocol that define the FU that should be used when approaching LCA of hydrogen production methods. The FU consists of 1 kg of H_2 with a purity >99%, final three-stage intercooled compression, a final pressure of 20 MPa, a temperature of 25 °C and 75% efficiency. However, although the choice of 1 kg of H_2 is the most common choice as FU, the final conditions in terms of the purity, final pressure and temperature are not usually adopted, hampering a definitive comparison.

Regarding the data quality, only three papers also considered the primary data from real plant operations or from pilot scale experiments, five used a software simulation to evaluate energy and material consumption, three do not specify the data collection process, while all the rest rely only on secondary data. The major source of secondary data across all the studies is the ecoinvent database (different versions were used, see Table 1), which was used in 14 works, both as the only data source or to integrate the inventory analysis in the case of a lack of information for specific processes. The sole recourse of the published literature and reports was adopted in two papers, while only one used the database integrated in the GaBi software version 10.5.1.124.

With respect to the software adopted to conduct the LCA, the most used is SimaPro (seven works), followed by GaBi and OpenLCA (three works each), whilst BrightWay was the least common (one works). For the remaining seven papers, no information was provided about the choice of the program.

Five different impact assessment calculation methods (LCIA) were found. The most used are CML 2001 and IPCC 2013 GWP 100a, which were adopted in five papers each, followed by the Environmental Footprint (E.F) and ReCiPe (four papers each). Out of the remaining three studies, one used the Impact 2002+ method, while for the last two, no specific information was provided.

Regarding system boundaries, most of the papers (16) refer to a "cradle-to-gate" approach, although it is not always specified which are the operating conditions in terms of annual production and/or the lifetime of the plant. Three papers limited the studies to "gate-to-gate", focusing the attention on the production process and excluding the raw material supply. Cradle-to-gate includes mass and energy flows from raw material extraction to the production phase, while gate-to-gate considers only the production steps that occur within the factory. Only one work also included the End-of-Life (EoL) stage by considering material recycling, incineration and landfilling from a water splitting Cu-Cl thermochemical plant powered by a concentrated solar power plant (CSP). Lastly, one paper does not specify the applied boundary condition. All the works refer to attributional LCA. In most cases, with hydrogen being the only output considered from the production process, no allocation was performed. Three papers adopted system expansion to compute the possible environmental benefits of using by-products generated within the plant as alternatives of new products available in the global market. Two papers used the cut-off approach, while mass or economic allocation were considered in one work each.

Table 1. LCA methodological aspects of the reviewed papers.

Ref.	Software	Type of Data	Background Database	F.U.	System Boundaries	LCIA
[22]	SimaPro 9.4	Secondary data	ecoinvent 3.5	1 kg H_2_harmonized	cradle-to-gate	E. F. 3.0
[23]	undefined	Secondary data	ecoinvent	1 kg H_2	cradle-to-gate	CML 2001
[24]	SimaPro	Secondary data	ecoinvent + literature + state of the art from producers	1 kg H_2	cradle-to-gate	E. F. 3.0
[25]	undefined	Software sim. + secondary data	Background data source + ecoinvent	1 kg H_2	cradle-to-gate	ReCiPe
[26]	undefined	Secondary data	ecoinvent	1 kg H_2, 80 bar, 10 °C	cradle-to-gate	IPCC 2013 GWP 100a
[27]	BrightWay 2 LCA	Secondary data	ecoinvent 3.7	1 kg H_2 80 bar	cradle-to-gate	IPCC 2013 GWP 100a
[28]	OpenLCA v 1.11	Secondary data	NETL Reports + literature	1 kg H_2, >99.9%; 925 psig	cradle-to-gate	IPCC 2013 GWP 100a; water balance
[29]	GaBi v 10.5.1.124	Secondary data	GaBi Database	1 kg H_2	cradle-to-gate	undefined
[30]	undefined	Secondary data	ecoinvent	1 kg H_2	cradle-to-gate	CML 2001
[31]	undefined	Secondary data	ecoinvent 3.8	1 kg H_2, 30 bar, 50 °C, 99.99% wt	undefined	E. F. 3.1
[32]	SimaPro 9.2	Secondary data	ecoinvent 3.5	1 kg H_2	cradle-to-gate	IPCC 2013 GWP 100a
[33]	GaBi	Primary (mining; fuel prep) + secondary data	Literature	1 kg H_2	cradle-to-gate	CML 2001
[34]	SimaPro 9.2	Secondary data	ecoinvent 3.8 + literature	1 kg H_2, 25 bar	cradle-to-gate	E. F. 3.0
[35]	GaBi 10	Secondary data	undefined	1 kg H_2	cradle-to-gate	ReCiPe
[36]	undefined	Software sim. + secondary data	Background data source + undefined secondary data	1 ton H_2; 1 MW power	cradle-to-gate	undefined
[37]	OpenLCA 1.10.2	Primary data (plant emission) + secondary data	undefined	1 kg H_2	gate-to-gate	ReCiPe
[38]	OpenLCA	Software sim. + secondary data	Background data source + Agribase + literature + ecoinvent	1 kg H_2 200 bar	gate-to-gate	Impact 2002+; AWARE
[39]	SimaPro 8.5.2	Software sim. + secondary data	Background data source + ecoinvent + GREET 2021	1 kg H_2	cradle-to-gate	ReCiPe 2016
[40]	SimaPro 9.13	primary (AD) + secondary data	ecoinvent 3.8	1 kg H_2; 99.99%	gate-to-gate	CML 2001
[41]	SimaPro 9.0	Software sim. + secondary data	Pilot scale + ecoinvent	1 kg H_2; 99.99%	cradle-to-gate	IPCC 2013 GWP 100a
[42]	undefined	Secondary data	undefined	1 kg H_2	cradle-to-grave	CML 2001

As can be seen from Table 1, the methodological choices vary across the studies. The FU, system boundaries and type of data used are the main parameters that can affect the final results, as well as the comparability among the different works. Hence, a common strategy should be implemented to ensure comparability among the different works.

Impacts across more than 20 different indicators were reported in the reviewed papers. However, in the present work, attention is focused only on the global warming potential (GWP), human toxicity (non-cancer), acidification potential and the depletion of abiotic resources (mineral). Three environmental indexes were selected among the recommended impact indicators suggested by the JRC [18], while human toxicity was chosen to try to evaluate which technology could be less harmful in terms of its direct impact on the population. In Table 2, the complete list of impact indicators and the number and percentage of papers in which they are used is reported.

Table 2. Impact categories used in the review papers.

Impact Category	N. of Papers	%
GWP	21	100%
Ozone depletion	8	38%
Ionizing radiation	5	24%
Phot. O3 form	5	24%
Ozone form., terr. Ecosyst	4	19%
Ozone form., human health	4	19%
Part. matter form	6	29%
Human tox., non-carc	9	43%
Human tox., carc.	8	38%
Acidification	13	62%
Eutroph. Freshwater	11	52%
Eutroph marine	4	19%
Ecotox terrestrial	6	29%
Ecotox freshw	7	33%
Marine Ecotox.	3	14%
Land use	5	24%
Water use	6	29%
Mat. Res., met/min	7	33%
Energy resources, non-ren	7	33%

From the 21 reviewed papers it was possible to derive a database of 104 different LCAs since, for comparison reasons, each work considers more than one technology at a time. The most investigated technologies are PEM (27 LCAs), SMR (24 LCAs: 14 SMR and 9 SMR + CCS), gasification (14 LCAs) and AE (10 LCAs), while the least investigated is AEM with only 1 LCA. The results were further aggregated according to the hydrogen color classification.

3.2. GHG Emissions

Great variation within the results of the GWP was found among the different technologies and system configurations. An overview of all the results, together with the relative technology adopted, the allocation method, the functional unit and the system boundaries, can be found in Table 3.

Table 3. GWP results of hydrogen production routes.

Technology	Allocation	F.U.	System Boundaries	kg_{CO2eq}/kg_{H2}	Ref.
AE_mono PV baseline	Not applicable	1 kg H_2 _harm.	cradle-to-gate	4.28	[22]
AE_mono PV updated				1.76	[22]
AE_multi PV baseline				3.78	[22]
AE_multi PV updated				1.83	[22]
AE_onshore	Not applicable	1 kg H_2	cradle-to-gate	0.11	[23]
AE_offshore	Not applicable	1 kg H_2	cradle-to-gate	0.92	[23]
AE_wind_base	Not applicable	1 kg H_2	cradle-to-gate	2.08	[24]
AE_wind_adv	Not applicable	1 kg H_2	cradle-to-gate	1.15	[24]
AE (Ita grid mix)	Not applicable	1 kg H_2	cradle-to-gate	4.32	[25]
AE + floating PV	Not applicable	1 kg H_2	cradle-to-gate	23.5	[25]
PEM_wind_base	Not applicable	1 kg H_2	cradle-to-gate	1.79	[24]
PEM_wind_adv	Not applicable	1 kg H_2	cradle-to-gate	1.03	[24]
PEM_wind (500 h/year)	Not applicable	1 kg H_2, 80 bar, 10 °C	cradle-to-gate	5.78	[26]
PEM_wind (4000 h/year)				0.73	[26]
PEM_PV (500 h/year)				9.45	[26]
PEM_PV (4000 h/year)				1.19	[26]
PEM_grid Crete	Cut off	1 kg H_2 80 bar	cradle-to-gate	41.4	[27]
PEM_hybrid Crete				27.4	[27]
PEM_grid Tenerife				21.6	[27]
PEM_hybrid Tenerife				12.6	[27]
PEM_grid Eigeroy				1.47	[27]
PEM_hybrid Eigeroy				1.26	[27]
PEM (US mix)	Not applicable	1 kg H_2, >99.9%; 925 psig	cradle-to-gate	31.3	[28]
PEM (PV)	Not applicable		cradle-to-gate	2.76	[28]
PEM (Wind)	Not applicable		cradle-to-gate	1.83	[28]
PEM-Solar	Not applicable	1 kg H_2	cradle-to-gate	2.50	[29]
PEM-Wind	Not applicable	1 kg H_2	cradle-to-gate	0.60	[29]
PEM + CSP	Not applicable	1 kg H_2	cradle-to-gate	8.67	[30]
PEM + PV	Not applicable	1 kg H_2	cradle-to-gate	9.37	[30]
PEM_onshore	Not applicable	1 kg H_2	cradle-to-gate	0.09	[23]
PEM_offshore	Not applicable	1 kg H_2	cradle-to-gate	0.89	[23]
PEM_EU grid	Not applicable	1 kg H_2, 30 bar, 50 °C, 99.99%	Undefined	2.37	[31]
PEM-BECCS (bio en + ccs)	Cut off	1 kg H_2	cradle-to-gate	−101.12	[32]
PEM nuclear	Cut off	1 kg H_2	cradle-to-gate	0.77	[32]
PEM Wind	Cut off	1 kg H_2	cradle-to-gate	2.05	[32]
PEM Hydro	Cut off	1 kg H_2	cradle-to-gate	3.25	[32]
PEM Solar	Cut off	1 kg H_2	cradle-to-gate	4.96	[32]
SOEC (US mix)	Not applicable	1 kg H_2, >99.9%; 925 psig	cradle-to-gate	25.2	[28]
SOEC (PV)	Not applicable		cradle-to-gate	2.93	[28]
SOEC (Wind)	Not applicable		cradle-to-gate	2.20	[28]

Table 3. *Cont.*

Technology	Allocation	F.U.	System Boundaries	kg_{CO2eq}/kg_{H2}	Ref.
Nuclear SOEC w/N2	Not applicable	1 kg H_2	cradle-to-gate	0.62	[33]
Nuclear SOEC without/N2	Not applicable	1 kg H_2	cradle-to-gate	0.21	[33]
SOEC_onshore	Not applicable	1 kg H_2	cradle-to-gate	0.21	[23]
SOEC_offshore	Not applicable	1 kg H_2	cradle-to-gate	1.49	[23]
PV_electrol 2019	Not applicable	1 kg H_2 25 bar	cradle-to-gate	3.90	[34]
PV_electrol 2050	Not applicable	1 kg H_2 25 bar	cradle-to-gate	1.40	[34]
Wind_electrol 2019	Not applicable	1 kg H_2 25 bar	cradle-to-gate	1.00	[34]
Wind_electrol 2050	Not applicable	1 kg H_2 25 bar	cradle-to-gate	0.50	[34]
Water el. + ren. e.e	Allocation by energy	1 kg H_2	cradle-to-gate	0.31	[35]
AEM_EU grid	Not applicable	1 kg H_2, 30 bar, 50 °C, 99.99%	undefined	2.42	[31]
BG	Not applicable	1 kg H_2, >99.9%; 925 psig	cradle-to-gate	5.31	[28]
BG + CCS	Not applicable	1 kg H_2, >99.9%; 925 psig	cradle-to-gate	−15.40	[28]
BG	Cut off	1 kg H_2	cradle-to-gate	1.11	[32]
BG + CCS	Cut off	1 kg H_2	cradle-to-gate	−13.80	[32]
CG	Not applicable	1 kg H_2, >99.9%; 925 psig	cradle-to-gate	20.00	[28]
CG + CCS	Not applicable	1 kg H_2, >99.9%; 925 psig	cradle-to-gate	3.92	[28]
Gasification–Coal Oxyfuel	Not applicable	1 ton H_2; 1 MW power	cradle-to-gate	11.00	[36]
Gasification–Plastic Oxyfuel	Not applicable	1 ton H_2; 1 MW power	cradle-to-gate	16.00	[36]
Gasification–Plastic Steam	Not applicable	1 ton H_2; 1 MW power	cradle-to-gate	40.00	[36]
Gasification–Plastic Air	Not applicable	1 ton H_2; 1 MW power	cradle-to-gate	24.00	[36]
SMR	Not applicable	1 ton H_2; 1 MW power	cradle-to-gate	10.00	[36]
SMR	Not applicable	1 kg H_2, >99.9%; 925 psig	cradle-to-gate	10.40	[28]
SMR-pipeline	Not applicable	1 kg H_2	cradle-to-gate	12.20	[29]
SMR-LNG	Not applicable	1 kg H_2	cradle-to-gate	13.40	[29]
SMR	Allocation by energy	1 kg H_2	cradle-to-gate	9.65	[35]
CH4 SMR	Not applicable	1 kg H_2	cradle-to-gate	12.60	[25]
SMR	Not applicable	1 kg H_2, 30 bar, 50 °C, 99.99%	undefined	10.80	[31]
SMR	Not applicable	1 kg H_2	gate-to-gate	9.35	[37]
SMR_2019	Not applicable	1 kg H_2 25 bar	cradle-to-gate	10.90	[34]
SMR_2050	Not applicable	1 kg H_2 25 bar	cradle-to-gate	10.60	[34]
SMR	Not applicable	1 kg H_2 200 bar	gate-to-gate	11.60	[38]
SMR	Cut off	1 kg H_2	cradle-to-gate	12.70	[32]
SMR + CCS-pipeline	Not applicable	1 kg H_2	cradle-to-gate	7.60	[29]

Table 3. *Cont.*

Technology	Allocation	F.U.	System Boundaries	kg_{CO2eq}/kg_{H2}	Ref.
SMR + CCS-LNG	Not applicable	1 kg H_2	cradle-to-gate	8.80	[29]
SMR + CCS	Allocation by energy	1 kg H_2	cradle-to-gate	3.78	[35]
SMR + CCS	Cut off	1 kg H_2	cradle-to-gate	5.62	[32]
SMR + CCS 2019	Not applicable	1 kg H_2 25 bar	cradle-to-gate	5.00	[34]
SMR + CCS 2050	Not applicable	1 kg H_2 25 bar	cradle-to-gate	4.20	[34]
SMR + CCS	Not applicable	1 kg H_2, >99.9%; 925 psig	cradle-to-gate	4.37	[28]
SMR-CCS	Not applicable	1 kg H_2 200 bar	gate-to-gate	7.70	[38]
CH4 SMR + CCS	Not applicable	1 kg H_2	cradle-to-gate	5.27	[25]
CH4_pyrolysis	Not applicable	1 kg H_2 200 bar	gate-to-gate	6.92	[38]
CH4 pyr-pipeline	Not applicable	1 kg H_2	cradle-to-gate	5.90	[29]
CH4 pyr-LNG	Not applicable	1 kg H_2	cradle-to-gate	8.10	[29]
H2S_pyrolysis	Not applicable	1 kg H_2 200 bar	gate-to-gate	5.25	[38]
MSW Pyrolysis + SMR	System expansion	1 kg H_2	cradle-to-gate	0.35	[39]
H2S_MR	Not applicable	1 kg H_2 200 bar	gate-to-gate	4.50	[38]
wPG (Waste Polym Gas)	Cut off	1 kg H_2	cradle-to-gate	9.75	[32]
wPG + CCS	Cut off	1 kg H_2	cradle-to-gate	1.34	[32]
MSW Pyrolysis + Gasif	System expansion	1 kg H_2	cradle-to-gate	21.5	[39]
MSW Gasification + WGS	System expansion	1 kg H_2	cradle-to-gate	26.7	[39]
bMtoH2	System expansion	1 kg H_2; 99.99%	gate-to-gate	1.54	[40]
Chem. loop.-iron based O2 carr	Allocation by energy	1 kg H_2	cradle-to-gate	1.01	[35]
Sorp. Enh. Ref_Ca sorbent	Allocation by energy	1 kg H_2	cradle-to-gate	1.77	[35]
Sorp. Enh. Ref_Ca sorbent + Cu bas O2 carr	Allocation by energy	1 kg H_2	cradle-to-gate	1.94	[35]
CSP + Cu-Cl water splitting	Not applicable	1 kg H_2	cradle-to-grave	0.94	[33]
Nuclear S-I	Not applicable	1 kg H_2	cradle-to-gate	0.31	[30]
bWtoH2	System expansion	1 kg H_2; 99.99%	gate-to-gate	2.13	[40]
MSW Landfill bior + SMR (heating w/hydro)	System expansion	1 kg H_2	cradle-to-gate	−31.70	[39]
MSW Landfill bior + SMR (react heat w/NG)	System expansion	1 kg H_2	cradle-to-gate	14.20	[39]
Enzym Hydrol + Fermentation	Economic allocation	1 kg H_2; 99.99%	cradle-to-gate	10.10	[41]
S-I cycle + CSP	Not applicable	1 kg H_2	cradle-to-gate	1.02	[30]

SMR is commonly used as a mature state-of-the-art process that can act as a benchmark to compare new hydrogen production technologies. Out of the 24 case studies evaluated, the GWP index was found to be in the range between of −31.68 kg_{CO2eq}/kg_{H2} and 14.16 kg_{CO2eq}/kg_{H2} [39]. Both results refer to an SMR process fed by landfill gas, coupled with the gasification of the extracted waste residues from the landfill bioreactor. The only difference between the two results lies in the source of electricity used to run

the system, which is supplied either by a hydropower plant (−31.68 kg_{CO2eq}/kg_{H2}) or by oil and gas-based fuels (14.16 kg_{CO2eq}/kg_{H2}). The authors refer that the negative value is due to the combined effect of using a renewable energy source with a low GWP (hydropower plant), together with a waste-derived feedstock to produce H_2. For this latter aspect, the avoided emissions that would have otherwise arisen from perpetual landfill were considered and entirely allocated to the produced hydrogen. Cho et al. [37] investigated SMR performance by using real emission data from 33 facilities in the US in a gate-to-gate approach, finding an average GWP of 9.35 kg_{CO2eq}/kg_{H2}, mostly due to the direct release of CO_2 during the process. When also considering the emissions coming from the methane supply chain (including leakage during extraction), the final GWP was found to be equal to 11.2 kg_{CO2eq}/kg_{H2}. In the same study, a further evaluation accounted for the possible use of landfill gas instead of NG. Conversely to what was previously reported by Wijayasekera et al. [39], the GWP could be reduced by up to 3.57 kg_{CO2eq}/kg_{H2} thanks to the avoided emissions during biogas production and gas flaring. Weidner et al. [34] also investigated the achievable emission reduction from now to 2050 considering the decarbonization pathways, finding a decrease of 2.8% and 14% in the GWP, respectively, for SMR and SMR + CCS. When comparing the medium values for SMR and SMR + CCS, the use of a carbon capture and storage system could provide a 50% reduction in the GHG emissions, while when analyzing the single case studies, the range is of 58−60% [25,28,35]. Figure 2 graphically reports the results for the GHG emissions of SMR and SMR + CCS. The x and the horizontal line inside each box represent, respectively, the mean and the median value, while the bottom and the top of the box express the 25th and 75th percentile, respectively. The whiskers extend up to the minimum and maximum value, where these are within the difference between the 75th and 25th percentile multiplied by 1.5. If minimum or maximum are below or above these thresholds, they are represented as point outside the whiskers.

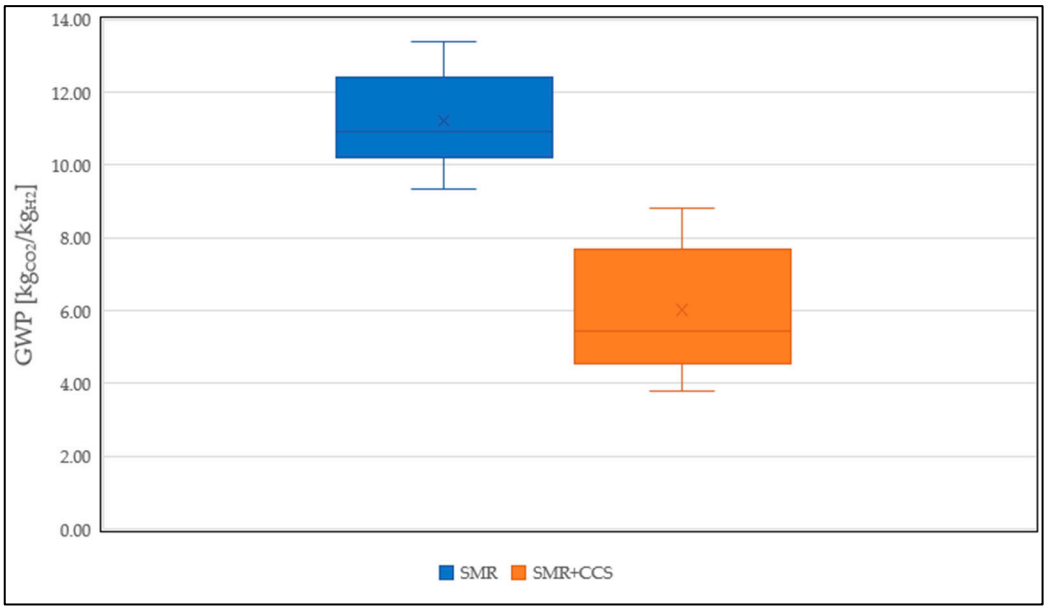

Figure 2. GWP of grey (SMR) and blue (SMR + CCS) hydrogen.

From the values reported in Table 3, the best and worst results are both associated with PEM electrolysis, with values of −101.12 kg_{CO2eq}/kg_{H2} [32] and 41.4 kg_{CO2eq}/kg_{H2} [27], respectively, in the case of using either bioenergy with CCS or the electric grid mix of Creta island. The authors refer to the fact that the negative value associated with PEM with bioenergy is due to the combination of a biogenic carbon energy source (wood chip) together with a CCS system. The cradle-to-gate boundary condition was considered in both studies, while the functional unit differs for the final hydrogen compression stage. The

use of grid energy also contributed to a higher GWP in the study of Henrsiksen et al. [28], which found an increase in emissions from 1.83 kg_{CO2eq}/kg_{H2} to 31.3 kg_{CO2eq}/kg_{H2} when supplying the same PEM stack either with wind or US grid mix energy. In [24], a PEM stack driven by wind energy or, when unavailable, by the Dutch grid generated 1.79 kg_{CO2}/kg_{H2}. Approximately 50% of emissions are due to the production of offshore wind electricity, 40% to the use of Dutch electricity mix, 8% to stack production and 2% to the BoP. The use of PV with PEM produced GHG emissions in the range of 1.19 kg_{CO2}/kg_{H2}–9.37 kg_{CO2}/kg_{H2} [30]. According to both Patel et al. [29] and Zhang et al. [30], the largest contribution to the GWP is attributed to solar plant construction, accounting for 96% and 78%, respectively. However, the absolute values differ significantly, accounting, respectively, for 2.4 kg_{CO2}/kg_{H2} and 7.3 kg_{CO2}/kg_{H2}. The recourse of a concentrated solar power (CSP) plant led to a total GWP of 8.67 kg_{CO2}/kg_{H2} [30]. The only work that assesses the use of a hydropower or nuclear plant together with a PEM stack [32] reports GHG emissions equal to 3.25 kg_{CO2eq}/kg_{H2} and 0.77 kg_{CO2eq}/kg_{H2}, respectively. In the graph of Figure 3, the results of the GHG emission of PEM in relation to the energy sources adopted are reported.

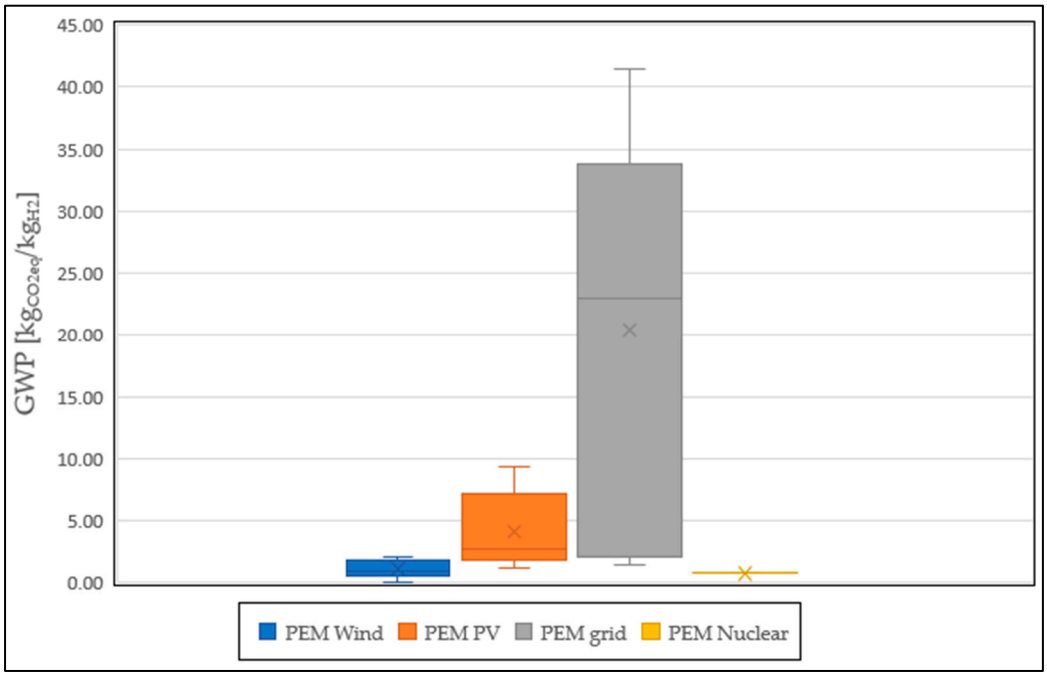

Figure 3. GWP of PEM stacks power by different energy sources.

Four papers investigated the eco-profile of Alkaline Electrolysis (AE) for a total of 10 case studies using either photovoltaic, wind or the electric grid as the energy source. While three LCAs refer to an FU of 1 kg_{H2}, Kolahchian Tabrizi et al. [22] used the harmonized protocol proposed by Valente et al. [21]. In [22], for a baseline scenario with outdated values of efficiency and process production for PV systems, the amount of GHG emissions for mono- and poly-PV AE are, respectively, 4.28 kg_{CO2eq}/kg_{H2} and 3.78 kg_{CO2eq}/kg_{H2}. The share of the impact related to the PVs covers almost all the emission (approx. 98%). At the same time, the authors found that when updating the values of PV technologies, impacts can be reduced by 59% and 52%, reaching a total GWP of 1.76 kg_{CO2eq}/kg_{H2} and 1.83 kg_{CO2eq}/kg_{H2} for mono- and poly-PVs, respectively. Higher results were reported by Mio et al. [25] for an alkaline electrolyzer fed either by a 100% Italian grid mix or by a floating PV plant supported by the grid when the solar source is unavailable. The grid mix was mainly based on the thermoelectric NG plant (44.3%), followed by hydropower energy (19.5%), PV (8.3%), wind (6.2%) and biofuels (5.6%); nuclear energy, coal and oil accounted, respectively, for 4.6%, 4.6% and 3.2%. The results show GHG emissions more than five times higher (23.5 kg_{CO2eq}/kg_{H2} against 4.32 kg_{CO2eq}/kg_{H2})

when using a floating PV plant instead of the grid mix. The use of wind energy was evaluated by both Zhang et al. [23] and Krishnan et al. [24], considering, respectively, onshore/offshore and baseline/advanced wind farms. For all the cases, the results were between 0.11 kg_{CO2eq}/kg_{H2} [23] and 2.08 kg_{CO2eq}/kg_{H2} [24].

Seven LCAs of SOEC systems were collected from three different papers [23,28,33] for cells that operate with energy coming from wind turbines, PV modules, the US grid or nuclear plants. Zhang et al. [23] reported a GWP of 0.21 kg_{CO2eq}/kg_{H2} and 1.49 kg_{CO2eq}/kg_{H2} for SOEC using electric energy produced, respectively, by onshore or offshore wind power plant, used to satisfy both the electrical and thermal requirements of the system. Henriksen et al. [28] found GHG emissions of 2.2 kg_{CO2eq}/kg_{H2} and 2.9 $kg_{CO2eq}/kg_{H2,}$ respectively, for wind- and PV-driven SOEC systems, with electricity being responsible for 65% and 74% of the emissions. The recourse of electric energy from the US grid raised GHG emissions by approximately one order of magnitude, reaching an overall value of 25.2 kg_{CO2eq}/kg_{H2}. Competitive results with wind-driven SOEC were achieved when recurring with nuclear power plant energy [33]. The work from Ji et al. benefits from the primary data for nuclear fuel production, while for the rest of the inventory, secondary data were used. The calculated GWP was 0.2 kg_{CO2eq}/kg_{H2} and 0.6 kg_{CO2eq}/kg_{H2}, respectively, in the case of the absence or presence of nitrogen in the feed stream. The major processes responsible for GHG emission are electrolysis cell manufacturing (27%), power plant construction (23%) and fuel disposal (22%), while the operation phase accounts for approximately 10%.

Five case studies were found about the LCA of water electrolysis, but without further specification of the technology adopted [34,35]. All works considered electric energy coming from renewable sources. Weidner et al. [34] reported the GWP for water electrolysis fed either by an offshore wind power plant or by a PV plant in two different scenarios: a 2019 or 2050 setup, finding that wind energy can ensure GHG emissions between 64% and 74% lower with respect to PV systems (1 kg_{CO2eq}/kg_{H2} against 3.9 kg_{CO2eq}/kg_{H2} for the 2019 scenario and 0.5 kg_{CO2eq}/kg_{H2} against 1.4 kg_{CO2eq}/kg_{H2} for the 2050 scenario). Chisalita et al. [35] calculated even lower emissions in the case of water electrolysis fed entirely by renewable energy, achieving 0.31 kg_{CO2eq}/kg_{H2}.

Hydrogen produced through AEM cells with electricity supplied by the EU grid presents GHG emissions of 2.42 kg_{CO2eq}/kg_{H2} [31]. From a hotspot analysis, during cell production, almost 90% of the GWP is due to the spraying process (33.99%), end plates (31.46%) and bipolar plates manufactory (23.32%). Within the spraying process, isopropanol is mainly responsible for the emission, accounting for 85% of the overall process. For the end plates, GHG emissions are due to their high mass share and the use of chromium steel that presents intense energy phases during both production and processing.

The results from the water split processes, either through the S-I or Cu-Cl cycle and coupled with a CSP plant, were reported, respectively, by Zhang et al. and by Sadeghi and Ghandehariu [30,42]. For the S-I cycle, the calculated GWP is 1.02 kg_{CO2eq}/kg_{H2}, mostly due to solar and hydrogen plant construction (0.78 kg_{CO2eq}/kg_{H2} and 0.21 kg_{CO2eq}/kg_{H2}, respectively), while impacts associated with the use phase of the hydrogen production plant are almost negligible. Cu-Cl cycles can provide a benefit of 8% lower emissions, reaching 0.94 kg_{CO2eq}/kg_{H2}, with a contribution of approximately 91% associated to solar plant construction. Impacts are mostly due to the significant amount of steel, iron, glass and molten salt used for plant manufactory. The operation phase accounts only for 0.041 kg_{CO2eq}/kg_{H2}, while hydrogen plant construction and assembly is responsible for 0.14 kg_{CO2eq}/kg_{H2}. The partial recycling of different materials of the CSP, with values in the range of 16–35%, allows a negative contribution to the overall GWP of -0.15 kg_{CO2eq}/kg_{H2}.

Gasification has been widely investigated for hydrogen production due to the possibility of using different inlet feedstock, both biogenic or not. As the share of hydrogen in the produced gas is not sufficient for direct utilization, usually, a high- and low-temperature water–gas-shift reactor and a pressure swing adsorber are considered at the exit of the gasifier. From the reviewed literature, a great variation of the GWP among the different processes was found, with values ranging from -15.4 kg_{CO2eq}/kg_{H2} [28] to

59.2 kg_{CO2eq}/kg_{H2} [39], respectively, in the case of biomass gasification with CCS and for the steam gasification of plastic wastes. The work in [39] reported a significant variation in the results when using hydropower electricity instead of traditional sources to power the system. In fact, the difference in emissions can be by even up to two orders of magnitude (59.1 kg_{CO2eq}/kg_{H2} against 0.59 kg_{CO2eq}/kg_{H2} in the case of oil and gas or hydropower electricity). Comparing the sole gasification with an integrated pyrolysis + gasification process, the latter scheme can drive to a GWP reduction of between 5% and 19%. GHG emissions for biomass gasification were found to be equal to 5.3 kg_{CO2eq}/kg_{H2} (−15.4 kg_{CO2eq}/kg_{H2} when coupled with CCS) [28], 1.1 kg_{CO2eq}/kg_{H2} (−13.8 kg_{CO2eq}/kg_{H2} with CCS) [32] and 1.5 kg_{CO2eq}/kg_{H2} [40], respectively, when using southern yellow pine, poplar wood, or bio-oil coming from the pyrolysis of sawmill by-products. The latter case is the only that refers to a gate-to-gate approach, not including the energy and material consumption for three cases of cultivation and harvesting, since the feedstock is considered as a by-product of a different system. Waste plastic gasification was studied by Salah et al. [32] and by Williams et al. [36] with different gasification agents. In [36], an equal share of waste plastic and biomass were gasified with either oxygen, air or steam, achieving a total GWP of 16 kg_{CO2eq}/kg_{H2}, 24 kg_{CO2eq}/kg_{H2} and 40 kg_{CO2eq}/kg_{H2}, respectively. A significantly lower value was calculated in [32] through the steam gasification of 100% waste polymers, finding GHG emissions of 9.7 kg_{CO2eq}/kg_{H2} and 1.3 kg_{CO2eq}/kg_{H2}, respectively, for gasification and gasification + CCS. In this case, the authors considered the avoided landfill or incineration of plastic wastes, accounting it for −2.4 kg_{CO2eq}/kg_{H2}, while no specific mentions were found in [36].

The pyrolysis of methane and/or hydrogen sulfide was also investigated, reporting GHG emissions between 4.5 kg_{CO2eq}/kg_{H2} and 8.1 kg_{CO2eq}/kg_{H2} [29,38]. Sole methane pyrolysis, when operated with shipped liquefied NG instead of pipelines NG, produces approximately 37% more CO_{2eq} emissions, raising them from 5.9 kg_{CO2eq}/kg_{H2} to 8.1 kg_{CO2eq}/kg_{H2}.

Promising results were reported for chemical looping technologies either with iron-based (Fe) or copper-based (Cu) oxygen carriers, which, respectively, generates 1.0 kg_{CO2eq}/kg_{H2} and 1.9 kg_{CO2eq}/kg_{H2}. Since processes rely on NG as a feedstock, 85% and 47% of the emissions are due to the gas supply chain, respectively, for Fe- and Cu-based O_2 carrier processes. The second major source of emissions is the hydrogen production section due to CO_2 treatment stages (drying and compression), which account for 6.3% and 42.6% of Fe-based and Cu-based O_2 carrier processes. The greater share for this latter case is mostly due to the partial decomposition of $CaCO_3$ in the calciner, which directly releases CO_2 into the environment.

The combination of biological processes, namely hydrolysis and fermentation, for food wastes (FW)'s conversion into hydrogen, was studied as a possible alternative to landfill disposal [41]. Out of the 10.1 kg_{CO2eq}/kg_{H2} generated, approximately 57% are due to gas compression, 17% to electricity consumption and 14% to FW transport (considered equal to 100 km with a 32 metric ton EURO5 truck). Avoided landfill contributed with −8.3 kg_{CO2eq}/kg_{H2}.

The following Figure 4 graphically reports the results of the presented studies, grouping the technologies according to the color classification commonly adopted. The average value of the SMR to be used as a reference benchmark to visualize the technologies that could guarantee lower emissions was also included. This latter parameter was calculated as the mean among all the GWP results for the SMR technology presented in Table 3. Water electrolysis systems were grouped in green, yellow and pink hydrogen, respectively, when coupled with energy coming from renewable sources, an electric grid or nuclear power plants. Blue and turquoise hydrogen refers, respectively, to SMR + CCS and methane pyrolysis. Waste and biomass/biowaste gasification are not included in any color classification, hence they were reported with the process definition name. For each technology, results that are significantly off-scale with respect to the general findings were excluded from the graph.

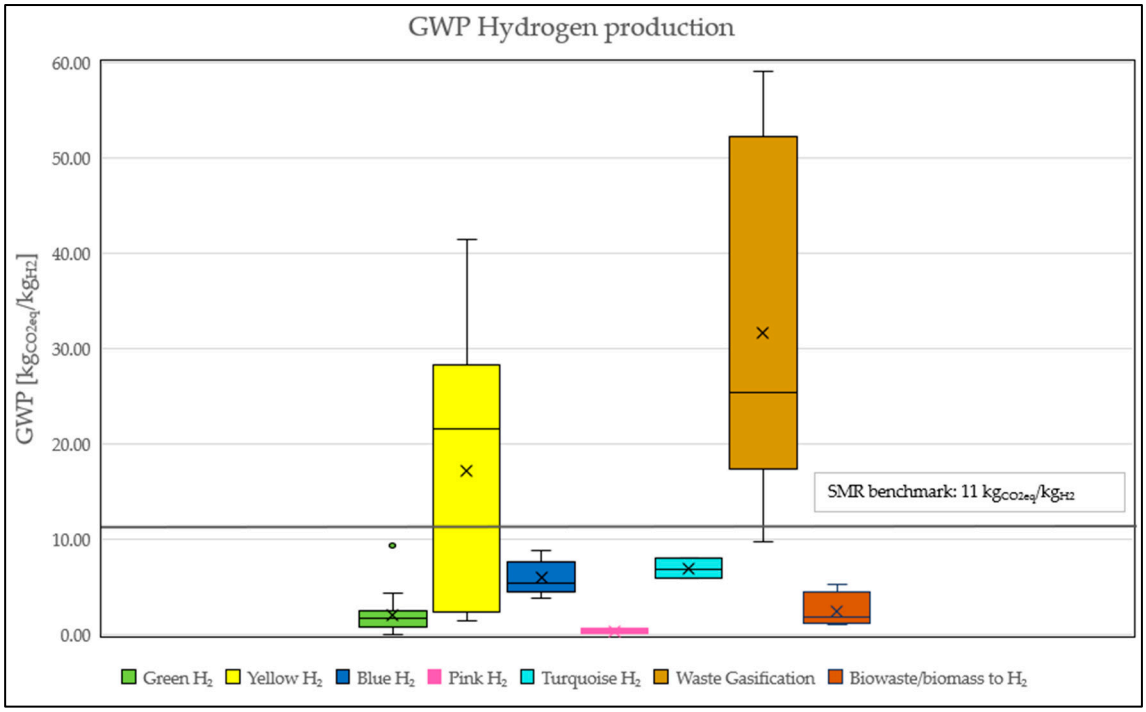

Figure 4. GWP impacts different hydrogen production routes.

3.3. Acidification Potential

The concept of the acidification potential refers to the deposition of acidifying agents onto various environmental compartments such as soil, groundwater, surface waters, living organisms, ecosystems and substances. Principal acidifying agents include sulfur dioxide (SO_2), nitrogen oxides (NOx) and ammonia (NHx). Acidifying agents instigate a broad spectrum of effects on soil quality, groundwater purity, surface water integrity, organismal health, ecosystem stability and material integrity.

Out of the 12 papers that report results for the acidification potential, two distinct unit measures were found. The most commonly used is kg_{SO2eq} which was found in 77% of the cases, while the rest adopted $molH^+_{eq}/kg_{H2}$. To facilitate a comparison, the results were only expressed as $molH^+_{eq}/kg_{H2}$ by using the conversion factor reported in [43]. The lowest and highest values were of 3.9×10^{-4} $molH^+_{eq}/kg_{H2}$ [30] and 2.2×10^{-1} $molH^+_{eq}/kg_{H2}$ [39], respectively, for onshore PEM and SMR with landfill biogas. Regarding water electrolysis, PEM presents values between 3.9×10^{-4} $molH^+_{eq}$ [30] and 4.4×10^{-2} $molH^+_{eq}/kg_{H2}$ [30] when coupled with onshore wind turbines or a CSP plant. From the seven LCAs reporting the AP values of PEM, it resulted in an average emission of 1.8×10^{-2} $molH^+_{eq}/kg_{H2}$. A similar trend was found for AE, with minimum and maximum emissions of 5.4×10^{-4} $molH^+_{eq}/kg_{H2}$ and 1.0×10^{-1} $molH^+_{eq}/kg_{H2}$, respectively, when using electric energy coming from an onshore wind power plant [23] or floating PV [25]. The calculated mean value was found equal to 1.8×10^{-2} $molH^+_{eq}/kg_{H2}$. The hotspot analysis reported in [24] showed that between 45% and 49% of the impacts are related to stack production, while the rest is almost entirely related to the energy supply. Regarding the stack components, the bipolar plate in AE cells is the major source of emissions (52% of the total) due to the high steel and nickel content. SOEC presents fewer scattered results than the other electrolysis technologies, with average emissions of 2.6×10^{-3} $molH^+_{eq}/kg_{H2}$, out of a minimum and maximum value of 7.8×10^{-4} $molH^+_{eq}/kg_{H2}$ and 6.0×10^{-3} $molH^+_{eq}/kg_{H2}$, respectively, when coupled with an onshore or offshore wind power plant [23]. The only work concerning AEM reports an acidification potential of 2×10^{-2} $molH^+_{eq}/kg_{H2}$ [31]. From the hotspot analysis of the cell, it results that almost 50% of the impacts are associated with bipolar plates, with the nickel supply being mainly responsible due to the emission of sulfur dioxide during

material extraction. This condition can also be found for the emission associated with Ni foam which, despite the reduced mass, accounts for 11.5% of the overall impacts associated with cell components. For PEM technology, the gold in the Porous Transport Layer (PTL) is present in the anode and cathode account for most of the impacts. Zhang et al. [23] reported also that when coupling electrolysis technologies with wind power systems, PEM can guarantee 40% and 102% lower emissions with respect to AE and SOEC, mostly due to the lower use of copper for cell manufactory and operation. For SOEC cells, Ji et al. [33] also reported that a significant source of emissions is the manufactory process of ferrochrome and yttrium oxide.

The S-I cycle and Cu-Cl water splitting, respectively powered by nuclear or CSP plants, reported an acidification potential of 1.2×10^{-3} $molH^{+}_{eq}/kg_{H2}$ [33] and 1.1×10^{-2} $molH^{+}_{eq}/kg_{H2}$ [42], respectively. The results from chemical looping technologies with either Fe- or Cu-based O_2 carriers present AP in the range of 1.4×10^{-3} $molH^{+}_{eq}/kg_{H2}$ and 3.1×10^{-3} $molH^{+}_{eq}/kg_{H2}$ [35].

For SMR, the impacts were in the range between 1.3×10^{-3} $molH^{+}_{eq}/kg_{H2}$ [35] and 1.6×10^{-2} $molH^{+}_{eq}/kg_{H2}$ [25], while the use of CCS led to an increase of 20%, with a total emission of 1.9×10^{-2} $molH^{+}_{eq}$ [25]. Between one and two orders of magnitude higher values of AP were found for the thermochemical treatment or process gases derived from MSW [39]. The gasification of bio-oil derived from the pyrolysis of sawmill waste biomass account for 4.2×10^{-3} $molH^{+}_{eq}/kg_{H2}$, mostly due to the sulfur emission associated with the production and use of the NG used in the reforming process and to the acid gases released during pyrolysis [40]. Lower emissions (4.0×10^{-4} $molH^{+}_{eq}/kg_{H2}$) were calculated in relation to the reforming of the biogas produced in an anaerobic digestion plant operating with biological wastes. In fact, the possible application of the digestate material as agricultural soil improver avoids the emission of acid that would have been otherwise generated for the production of fertilizers [40]. The following Figure 5 shows the trend in acidification potential for all the different technologies.

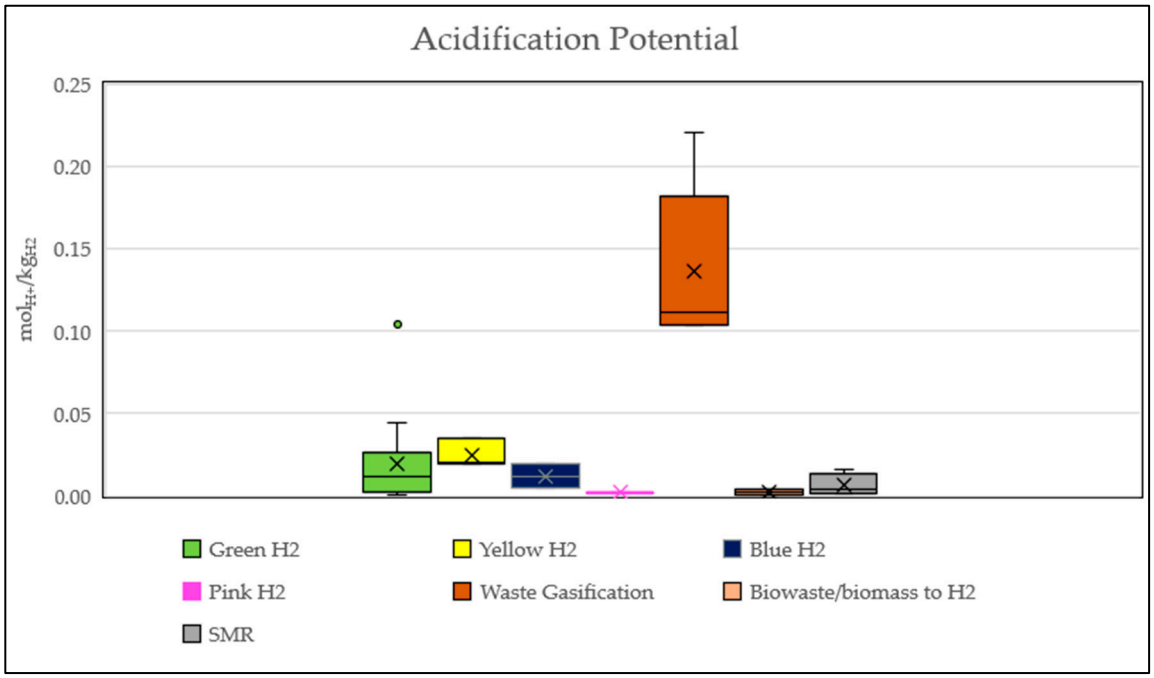

Figure 5. Acidification Potential for different hydrogen production routes.

3.4. Material Depletion

Material depletion is one of the two categories that are generally included in the Abiotic Depletion Potential (ADP) and it is commonly measured either in kg_{Sbeq} or in kg_{Cueq}, according to the impact category assessment method used. Eight papers reported

the material depletion potential, six using Antimony as the reference material, while the remaining two refer to Copper. According to Tabrizi et al., AE coupled with a PV power plant resulted in 1×10^{-4} kg_{Sbeq}/kg_{H2} and 1.1×10^{-4} kg_{Sbeq}/kg_{H2}, respectively, in the case of mono- and polycrystalline PV plants [22], while Mio et al. refer to 5.1×10^{-2} kg_{Cueq}/kg_{H2} both in the cases of the energy supplied through a floating PV plant or the EU grid [25]. The work conducted by Krishnan et al. reported lower impacts when using wind energy, achieving an index of material depletion of 5.6×10^{-5} kg_{Sbeq}/kg_{H2} [24]. From the hotspot analysis of the stack components, it resulted that 51.8% of the impacts are associated with the manufactory of the bipolar plate, 33.2% to the anode, while the cathode and end plate accounted, respectively, for 13.1% and 1.2% [24]. Similarly, also for PEM cells, the highest impacts shared are associated with the production of the bipolar plate (65.6%), followed by the PTL which accounted for 23.4%, while 8.1% are associated with the anode. The cathode and end plate account, respectively, for 2.8% and 0.1% [24]. As previously reported for AE, and also for PEM, a significant reduction in the impacts (≅50%) can be achieved when passing from the EU grid [31] to wind energy [24] (2×10^{-4} kg_{Sbeq}/kg_{H2} against 9.8×10^{-5} kg_{Sbeq}/kg_{H2}). A critical material assessment conducted by Schropp et al. [31] reported a more severe condition for PEM, with respect to AEM, mostly due to the use of Iridium and Titanium during cell production. In the same paper, the material depletion for AEM is reported as being equal to 2×10^{-4} kg_{Sbeq}/kg_{H2}, together with an impact repartition in relation to the manufacturing process. On a percentage basis, the highest impact share is due to the bipolar plate (26.8%), despite its lower mass with respect to the end plate, which instead accounts for 25%. Similarly, the NiMo catalyst, although it accounts for less than 1% in its mass share, it is responsible for 10.4% of the final impact, almost entirely due to the presence of the molybdenum.

Two papers also analyzed the ADP for SMR, finding values of 2.5×10^{-3} kg_{Cueq}/kg_{H2} and 7.8×10^{-3} kg_{Cueq}/kg_{H2} [25,35]. When integrating the system with a CCS, increases in the impacts by 8% and 34% were found. However, the reuse of the sorbent in cement factories could reduce impacts by approximately 13% [35].

Pyrolysis, gasification and integrated pyrolysis with the gasification of MSW resulted in 3×10^{-3} kg_{Cueq}/kg_{H2}, 4×10^{-3} kg_{Cueq}/kg_{H2} and 5×10^{-3} kg_{Cueq}/kg_{H2}, respectively, with reactors heated through NG and electric energy coming from a thermoelectric power plant [39]. Integrated pyrolysis and gasification were also studied by Arfan et al. [40] using waste biomass derived from a sawmill plant, resulting in 1.1×10^{-5} kg_{Sbeq}/kg_{H2}. The authors report that more than 50% of the impact is related to the reforming process of pyrolysis oil, due to the use of NG. Coupling steam reforming with the anaerobic digestion of biowaste led to a negative impact equal to -1.8×10^{-5} kg_{Sbeq}/kg_{H2}, thanks to the use of digestate that replaces fertilizer production [40]. These latter results are the only one referring to gate-to-gate system boundaries, while in all the others, it was considered a cradle-to-gate.

3.5. Human Toxicity Non-Cancer

Nine papers evaluated the non-carcinogen human toxicity of different hydrogen production routes. In most of cases (four papers), the authors refer to $kg_{1,4DCBeq}$.Two further unit measurements were found, expressing the impacts in CTUh and g_{DCBeq}. One paper refers to generic human toxicity potential, without a distinction among carcinogens and non-carcinogens.

When expressing the impacts through CTUh, comparable results were found for wind-driven AE and PEM, reporting, respectively, 3.99×10^{-8} and 4.05×10^{-8} $CTUh/kg_{H2}$ [24]. Most of the impacts are associated with the electricity supply, which accounts for 80% and 87%, respectively, for AE and PEM, mostly due to the intensive use of copper. Impacts shared for stack production are in the range of 12–19%. In AE cells, around 50% of stack impacts are related to the bipolar plate, 28% to the anode and 17% to the cathode. In PEM, the anode and bipolar plate account approximately for 35% each, 19% is associated to the PTL and 12% to the cathode. The presence of nickel, and to a lower extent, of steel, in the bipolar

plate and electrode, is the major source of impacts. For both technologies, BOP and PE account for less than 1.5%. The use of EU grid electricity instead of wind raises the impacts of PEM by approximately one order of magnitude, resulting in 1.3×10^{-7} CTUh/kg_{H2} [31]. A similar trend was found for AE with PV energy instead of wind, which turned into an increase in impacts up to 1.5×10^{-7} CTUh/kg_{H2} [22]. The analysis of AEM coupled with EU grid electricity accounted for 1.3×10^{-7} CTUh/kg_{H2}, with more than 95% of the impacts related to electricity production [31]. Considering only the cell itself, the end plates are responsible for the vast majority of impacts (34.1%), followed by the bipolar plates (26.5%), and the spraying process (22.4%). A better performance can be achieved with SMR, with a human toxicity impact of 2×10^{-8} CTUh/kg_{H2} [31].

Considering the studies that refers to $kg_{1,4DCB\_eq}$, a significant discrepancy among the results was found regarding for SMR. The lowest value was found by Cho et al. [37], reporting a final impact of 1.5×10^{-3} $kg_{1,4DCB\_eq}/kg_{H2}$. Between one and two orders of magnitude higher values were calculated by Chisalita et al. [35] and Mio et al. [25] in a cradle-to-gate analysis, finding emissions of 3.2×10^{-2} $kg_{1,4DCB\_eq}/kg_{H2}$ and 9.1×10^{-1} $kg_{1,4DCB\_eq}/kg_{H2}$, respectively. The integration with a CCS system further raised the impacts between 19% and 81%.

Chemical looping with an Fe-based O_2 carrier and sorption-enhanced reforming with Ca-based sorbent, used with or without a copper-based O_2 carrier, reported impacts of 3.5×10^{-2} $kg_{1,4DCB\_eq}/kg_{H2}$, 4.7×10^{-2} $kg_{1,4DCB\_eq}/kg_{H2}$ and 4.8×10^{-1} $kg_{1,4DCB\_eq}/kg_{H2}$, respectively [35]. For the first case, almost all the impacts are associated with the NG supply chain and wastewater treatment, accounting respectively for 71.6% and 25.5%. For sorption enhanced chemical looping with Cu based O_2 carrier, more than 90% of the final impacts are related to the CuO supply chain, 6% to NG supply, and 2% to the waste water treatment. Negative values were reported by both Arfan et al. [40] and Wijayasekera et al. [39], in case of thermochemical processes of either organic or MSW. In [40], the gate-to-gate analysis resulted in -2.7×10^{-1} $kg_{1,4DCB\_eq}/kg_{H2,}$ thanks to the avoided emissions resulting from the use of liquid digestate as an alternative to the production of fertilizers. In fact, the system expansion approach allowed to account for material and energy consumption, as well as harmful emissions (N-compounds, phosphate, or heavy metals), that would had been otherwise associated to the production of biofertilizer. Hence, these impacts were subtracted from the results of the hydrogen production process, comporting negative emission values. The work of Wijayasekera et al. [39] encompasses 32 different scenarios in cradle-to-gate system boundaries but, considering NG for reactor heating and transportation fuel, together with electricity produced from oil and gas, impacts resulted to be in the range from -4×10^{-1} $kg_{1,4DCB\_eq}/kg_{H2}$ to -1.7×10^{-1} $kg_{1,4DCB\_eq}/kg_{H2}$.

The nuclear-based S-I cycle and SOEC hydrogen production were found to have comparable emissions ranging from 1.1×10^{-1} $kg_{1,4DCB\_eq}/kg_{H2}$ to 1.4×10^{-1} $kg_{1,4DCB\_eq}/kg_{H2}$ [33]. In both cases, hydrogen plant construction resulted in being the main contributor to the overall impacts. The highest impacts reported in $kg_{1,4DCB\_eq}/kg_{H2}$ are related to AE fed wither with Italian grid mix or floating PV which accounted, respectively, for 1.2×10^{1} $kg_{1,4DCB\_eq}/kg_{H2}$ and 1.8×10^{1} $kg_{1,4DCB\_eq}/kg_{H2}$ [25].

4. Discussion

From the graph reported in Figure 4, a significant variation among the different hydrogen-producing technologies can clearly be seen in terms of the results' consistency, with respect to the calculated GHG emissions. In fact, while for green, blue, turquoise, and biomass/biowaste gasification, results are within a limited range of variation, yellow and waste gasification hydrogen are much more scattered. To better define trends, the mean values and standard deviation, together with the number of LCAs for each category, are reported in the following Table 4.

Table 4. Mean values and standard deviation of GWP for the main hydrogen production routes based on the reviewed papers.

	Green H_2	Yellow H_2	Blue H_2	Pink H_2	Turquoise H_2	Waste Gasif.	Biow./Biom. Gasif
Mean [kg_{CO2eq}/kg_{H2}]	2.02	17.20	6.02	0.41	6.97	33.90	2.52
St. dev. [kg_{CO2}/kg_{H2}]	1.99	14.90	1.79	0.29	1.10	18.50	1.90
num. LCAs	22	9	8	2	4	11	4

When considering hydrogen produced from electrolyzers, the eco-profile of the system is predominantly influenced by the use phase, making it strongly dependent on the adopted energy source. In fact, the use of grid energy can lead toward significant differences in GHG emissions due to the level of dependency from fossil thermoelectrical power plants. This condition can clearly be seen by comparing the results obtained by Terlouw et al. [27], when considering a PEM stack installed, respectively, in Creta or in Eigeroy island, with the first being almost 30 times higher than the latter (41.4 kg_{CO2eq}/kg_{H2} against 1.5 kg_{CO2eq}/kg_{H2}). The reason for this difference lies in the intense use of fossil fuels for energy production in Creta island, while in Eigeroy, most of the energy is produced by wind farms. However, this paper lacks a specific definition of the grid mix and the proportion of each energy source utilized for power generation (natural gas, coal, wind, etc.), reporting instead only the overall GHG intensity of the grid. Additional details, such as the reference year and the share of different energy sources, should always be included when addressing grid mix electricity to ease the interpretation of the results. The results from Mio et al. [25], regarding the use of an AE stack with the Italian energy grid mix, are closer to the lower value due to the significant share of electricity produced from renewable sources (≅43%) and the low recourse of coal and oil in thermoelectrical plants (>8% of the total e.e. produced). Similarly, Krishnan et al. [24] found that for wind-driven PEM and AE systems, the recourse of grid energy when the natural source is unavailable accounts for 40% and 56% of the final GWP, respectively. To a lesser extent, also when dealing with only renewable sources for energy supply, the results can present major variations. In fact, when comparing the results reported by Chisalita et al. [35] and Weidner et al. [34], the effect of a different energy mix used to supply energy to water electrolysis systems can be seen. As reported in Table 3, when passing from a PV or wind-driven system to an electric mix composed of 64.4% hydropower, 28.5% wind and 7% PV, emissions can be reduced by, respectively, 92% and 69%. The use of an offshore wind power plant instead of one onshore for green hydrogen production can also have a significant contribution in increasing the GWP. In fact, emissions can be raised by 6 to 8.5 times [23], mostly due to the higher effort and consumptions associated with offshore plants, which present more difficulties during plant construction and the need to withstand the corrosive marine environment, raising the environmental burdens. However, due to the very low emissions of the onshore system (0.09 kg_{CO2eq}/kg_{H2}–0.2 kg_{CO2eq}/kg_{H2}), the final results fall entirely in the confidence range of the green hydrogen production routes.

When dealing with gasification processes, the choice of the gasification agent, as well as the differences in the feed stream to the gasifier, significantly contribute to building up the gap among the different studies. The contribution due to the use of different gasification agents can clearly be seen in the work of Williams et al. [36], which reported results between 16 kg_{CO2eq}/kg_{H2} and 40 kg_{CO2eq}/kg_{H2} when passing from oxygen to steam in a plastic + biomass gasification process. Moreover, the differences in plant complexity (number of reactors for water gas shift reaction, compression stages, auxiliary boilers or the use of heat recovery and furnace for tail gases) enhanced the gap among the different studies.

Regarding SMR, although all the studies converge to similar results, variations in the GWP in the range of 10–20% can be found when including CH_4 leakage during extraction and transport [37,44,45]. In fact, despite different authors referring to the fact that CH_4

leakages are negligible when accounting for the overall GHG emissions [29,46], they usually refer to the incidence of fugitive gas that occurs only within the SMR plant.

With respect to H_2S pyrolysis, the addition of hydrogen sulfide in the methane pyrolysis process can reduce CH_4 consumption by up to one third, while maintaining the same hydrogen output. This condition, together with null CO_2 direct emission during the process, makes the technology appealing in terms of the GWP. In fact, CO_2 is only indirectly produced for process heating and electricity consumption, with this latter accounting for 40–50% of GHG when coupled with the energy coming from the EU grid. The major drawbacks in H_2S utilization are related to its high toxicity and the lack of worldwide availability. This latter criticality presents a further limit to H_2S pyrolysis due to the need of 17 kg of H_2S for each kg of H_2 produced.

GHG emissions from hydrolysis and the fermentation of food waste were calculated considering an impact allocation made on an economic basis, with hydrogen being only one of the produced outputs of the system (also including CO_2 and undigested material) and ascribing to H_2 53.3% of the total GWP. Through a sensitivity analysis, the authors also considered three other different allocation methods, namely: mass allocation, system expansion and no allocation. In the case of mass allocation, due to the very low mass share of H_2 in the output products (hydrogen accounts only for 0.6% w/w), the GWP would be reduced by up to 0.11 kg_{CO2eq}/kg_{H2}. When considering system expansion, a raise of 8.9% was found in the GWP with respect to economic allocation. In this case, the authors considered that undigested food waste could be used to produce fish feed, replacing crop-derived material. For "no allocation", all the impacts were attributed to the production of H_2, resulting in the highest emissions (18.9 kg_{CO2eq}/kg_{H2}). In terms of the mass balance, 1 kg of H_2 can be produced from approximately 284 kg of food waste, hence significant other output is produced by the plant.

As can be seen from Figure 5 and Table 5, the main differences in trends for AP, with respect to the GWP, are associated to green, yellow and blue hydrogen. In fact, the recourse to renewable energy systems to power electrolyzers plays a minor role with respect to cell production in the acidification potential, decreasing the gap between green and yellow hydrogen. Moreover, the more scattered results for green hydrogen reflect the AP trend associated with wind and solar (PV and CSP) systems, with the latter resulting in emissions even two orders of magnitude higher than the former. The higher complexity of the blue hydrogen production routes with respect to standard SMR is reflected also in an increase in the AP, which results in 50% higher emissions on an average basis. No specific analysis on the results from the other production pathways can be derived due to a lack of information in the original papers. This condition is often encountered for most of the impact indicators, except for the GWP. In fact, the vast majority of the papers used in the present review, despite reporting results for numerous impact categories, only analyze GHG emissions without addressing any information about the others.

Table 5. Mean values and standard deviation of AP for the main hydrogen production routes based on the reviewed papers.

	Green H_2	**Yellow H_2**	**Blue H_2**	**Pink H_2**	**Waste Gas**	**Biow/Biom to H_2**	**SMR**
Mean [mol_{H+}/kg_{H2}]	0.019	0.025	0.012	0.0018	0.14	0.0023	0.0061
St. dev. [mol_{H+}/kg_{H2}]	0.029	0.0087	0.017	0.0011	0.049	0.0027	0.0067
num LCAs	13	3	2	2	5	2	4

The results from material depletion and human toxicity hamper a definitive comparison among the works due the different unit measurements adopted, which are derived from different LCIA methods. This is a condition that is often encountered when approaching an LCA comparison that still needs to be properly tackled. Aside from the harmonized conditions relative to the choice of LCA parameters (FU, system boundaries, H_2 purity

level and final pressure) that were proposed by Valente et al. [21] to obtain comparable results for hydrogen production routes, the standardization of the unit measurements used for impact indicators could probably also ease the final comparison.

5. Conclusions

The present review analyzes the life cycle environmental impacts of different hydrogen production routes by focusing attention on four impact indicators. With respect to the GWP, green, blue, turquoise and pink hydrogen, together with biomass/biowaste for hydrogen processes, can perform better that SMR. For yellow H_2, the results show scattered behavior, performing better or worse according to the dependence of the electric grid on fossil-fuel-based power plants and the reference year of the energy mix used for the calculations. The trend toward a decarbonized energy production scenario will definitely reduce the gap among green and yellow hydrogen, making this latter a valid option to produce hydrogen with a reduced impact on climate change. However, considering the mean value coming from the analyzed literature published until now, the process still performs worse than SMR. Nevertheless, it should be noted that, despite the recent publication dates of the analyzed literature, in many cases, the reference year of the grid mix adopted is not specified. Therefore, the results may reflect a past condition that does not account for the most recent progress toward decarbonization. Waste gasification seems to be the less environmentally friendly among the processes studied, with more scattered results due also to the significant differences between the proposed plant configuration and the variability of the inlet feedstocks. The use of a residual biomass and biowaste seems an appealing solution to reduce GHG emissions, although it needs to be considered within a more complex picture that also includes by-products' allocation, since hydrogen represents only a share of the final products. S-I and Cu-Cl processes coupled with CSP plants also reported considerably lower impacts than SMR.

The acidification potential trend shows similar patterns with respect to the GWP, but with lower differences between yellow and green H_2 due to the contribution associated with renewable energy systems. In fact, the processes related to PV and wind farm production account for materials that raise the environmental burdens, lowering the benefits that can be achieved with respect to only GHG emissions. Blue hydrogen showed a slightly worse performance than grey due to the contribution associated with the CCS system.

The hotspot analysis reveals that for electrolysis processes, aside from the strict dependency on the electricity source consumed during the use phase, the material selection for cell production plays a fundamental role in all the impact categories analyzed. Nickel and gold are mainly responsible for AP in AEM and PEM, respectively, while for the ADP, Iridium and Titanium should be given particular attention. The ADP presents significantly more relevance to the electrolysis processes due to the strict dependency on noble and non-noble materials or, in general, to low-abundance elements. In fact, all the LCAs applied to these technologies adopted a cradle-to-gate approach to also include the impacts associated with material extraction and processing in the computation. However, the lack of fully established recycling processes for electrolysis technologies hampers the recovery of precious materials that could mitigate the impacts on the ADP. In fact, almost all of the LCAs on hydrogen production methods do not account for the EoL stage due to the shortage of reliable information about specific technologies. At present, most of the processes for the recovery of platinum group metals present a low Technology Readiness Level and elevated cost and energy demands, employ hazardous precursors and emit toxic and corrosive compounds. Also, the recycling of coated metals from a metal surface still faces several challenges and is far from being technically available [24]. Among the reviewed literature, only one paper considered the EoL stage, but it refers only to the material recovery of the energy production system used to supply electricity to the electrolysis stack. However, there is increasing attention toward the possible strategies to recycle critical materials from a circular economy perspective, although the benefits could be seen in a few decades from today [47–49]. It is very likely that the inclusion of recycling processes

will change the environmental burdens and the hotspot related to hydrogen production technologies, but as long as there is no industrially available technology, the extent cannot be properly evaluated.

From a methodological standpoint, the lack of a standardized procedure regarding the choice of the functional unit, system boundaries, cut off and allocation methods hamper a definitive comparison among the results of different studies. Within the literature reviewed, the main differences lie in the choice of the functional unit. Indeed, in most cases it is not specified which is the final condition in terms of the temperature and pressure of the produced hydrogen, making it more difficult to compare the eco-profiles. Impact allocation is usually entirely attributed to hydrogen, mostly when dealing with electrolysis processes since the O_2 produced is vented into the atmosphere. However, in the case of processes that generate valuable by-products as the fertilizer from the AD, system expansion or economic allocation should be considered.

A significant limit of the reviewed literature is that in most cases there is a considerable lack of information regarding the hotspot of the processes and the performance of many of the impacts, except for the GWP. More efforts should be made in this sense to define the burdens of hydrogen production technologies across all the environmental indicators. The use of rare earth materials and other low-abundance minerals will play a fundamental role in the possible development of energy-related processes like hydrogen production, but could influence geopolitical aspects of the producing countries at the same time. Moreover, water consumption for energy purposes could affect availability for human and agricultural consumption in arid regions of the globe. These aspects should be more accounted for in future research to define a more complete panoramic of the impacts associated with hydrogen production and to propose strategies to mitigate them.

Author Contributions: Conceptualization, M.P.M., M.F. and M.C.; writing—original draft preparation, M.P.M. and M.F.; writing—review and editing, M.F., M.P.M., M.C., S.L. and G.M. All authors have read and agreed to the published version of the manuscript.

Funding: Funded by the Italian Ministry of Environment and Energy Security in the framework of the Mission Innovation Initiative Challenge 8 "Renewable and Clean Hydrogen" Project "Hydrogen demo Valley: Infrastrutture polifunzionali per la sperimentazione e dimostrazione delle tecnologie dell'idrogeno".

Data Availability Statement: Not applicable.

Conflicts of Interest: The authors declare no conflicts of interest.

Abbreviations

ADP	Abiotic Depletion Potential
AD	Anaerobic Digestion
AE	Alkaline Electrolysis
AEM	Anion Exchange Membrane
AP	Acidification Potential
BECCS	Bioenergy with Carbon Capture and Storage
BG	Biomass Gasification
bMtoH2	Biomass to Hydrogen
bWtoH2	Biowaste to Hydrogen
CCS	Carbon Capture and Storage
CG	Coal Gasification
CSP	Concentrated Solar Power
EU	European
FU	Functional unit
GHG	Greenhouse gas
GWP	Global Warming Potential
HTP	Human Toxicity Potential
LCA	Life Cycle Assessment

LCI	Life Cycle Inventory
LCIA	Life Cycle Impact Assessment
MSW	Municipal Solid Waste
PEM	Proton-Exchange Membrane
PTL	Porous Transport Layer
PV	Photovoltaic
NG	Natural Gas
LNG	Liquefied Natural Gas
SMR	Steam Methane Reforming
SOEC	Solid Oxide Electrolyzer Cell
wPG	Waste Plastic Gasification

References

1. Intergovernmental Panel on Climate Change Technical Summary. In *Climate Change 2021—The Physical Science Basis*; Cambridge University Press: Cambridge, UK, 2023; pp. 35–144.
2. European Hydrogen Observatory. Available online: https://observatory.clean-hydrogen.europa.eu/hydrogen-landscape/production-trade-and-cost/hydrogen-production (accessed on 27 February 2024).
3. IEA. *Global Hydrogen Review 2023*; IEA: Paris, France, 2023.
4. Chelvam, K.; Hanafiah, M.M.; Woon, K.S.; Ali, K. Al A Review on the Environmental Performance of Various Hydrogen Production Technologies: An Approach towards Hydrogen Economy. *Energy Rep.* **2024**, *11*, 369–383. [CrossRef]
5. Borges, P.T.; Sales, M.B.; César Guimarães, C.E.; de França Serpa, J.; de Lima, R.K.C.; Sanders Lopes, A.A.; de Sousa Rios, M.A.; Desai, A.S.; da Silva Lima, A.M.; Lora, E.E.S.; et al. Photosynthetic Green Hydrogen: Advances, Challenges, Opportunities, and Prospects. *Int. J. Hydrogen Energy* **2024**, *49*, 433–458. [CrossRef]
6. Teke, G.M.; Anye Cho, B.; Bosman, C.E.; Mapholi, Z.; Zhang, D.; Pott, R.W.M. Towards Industrial Biological Hydrogen Production: A Review. *World J. Microbiol. Biotechnol.* **2024**, *40*, 37. [CrossRef] [PubMed]
7. González-Arias, J.; Zhang, Z.; Reina, T.R.; Odriozola, J.A. Hydrogen Production by Catalytic Aqueous-Phase Reforming of Waste Biomass: A Review. *Environ. Chem. Lett.* **2023**, *21*, 3089–3104. [CrossRef]
8. Busch, P.; Kendall, A.; Lipman, T. A Systematic Review of Life Cycle Greenhouse Gas Intensity Values for Hydrogen Production Pathways. *Renew. Sustain. Energy Rev.* **2023**, *184*, 113588. [CrossRef]
9. Wilkinson, J.; Mays, T.; McManus, M. Review and Meta-Analysis of Recent Life Cycle Assessments of Hydrogen Production. *Clean. Environ. Syst.* **2023**, *9*, 100116. [CrossRef]
10. Singh, S.; Pandey, G.; Rath, G.K.; Veluswamy, H.P.; Molokitina, N. Life Cycle Assessment of Biomass-Based Hydrogen Production Technologies: A Review. *Int. J. Green Energy* **2023**, 1–16. [CrossRef]
11. Morya, R.; Raj, T.; Lee, Y.; Kumar Pandey, A.; Kumar, D.; Rani Singhania, R.; Singh, S.; Prakash Verma, J.; Kim, S.-H. Recent Updates in Biohydrogen Production Strategies and Life–Cycle Assessment for Sustainable Future. *Bioresour. Technol.* **2022**, *366*, 128159. [CrossRef]
12. Masilela, P.; Pradhan, A. Systematic Literature Review of the Sustainability and Environmental Performance of Dark Fermentative Biohydrogen Production. *J. Clean. Prod.* **2022**, *372*, 133541. [CrossRef]
13. Nandhini, R.; Berslin, D.; Sivaprakash, B.; Rajamohan, N.; Vo, D.-V.N. Thermochemical Conversion of Municipal Solid Waste into Energy and Hydrogen: A Review. *Environ. Chem. Lett.* **2022**, *20*, 1645–1669. [CrossRef]
14. Hermesmann, M.; Müller, T.E. Green, Turquoise, Blue, or Grey? Environmentally Friendly Hydrogen Production in Transforming Energy Systems. *Prog. Energy Combust. Sci.* **2022**, *90*, 100996. [CrossRef]
15. Hosseinzadeh, A.; Zhou, J.L.; Li, X.; Afsari, M.; Altaee, A. Techno-Economic and Environmental Impact Assessment of Hydrogen Production Processes Using Bio-Waste as Renewable Energy Resource. *Renew. Sustain. Energy Rev.* **2022**, *156*, 111991. [CrossRef]
16. Özen Daş, İ.T.; Özmıhçı, S.; Büyükkamacı, N. Environmental Impact Analysis of Different Wastes to Biohydrogen, Biogas and Biohytane Processes. *Int. J. Hydrogen Energy* **2024**, *56*, 1446–1463. [CrossRef]
17. Hassan, N.S.; Jalil, A.A.; Rajendran, S.; Khusnun, N.F.; Bahari, M.B.; Johari, A.; Kamaruddin, M.J.; Ismail, M. Recent Review and Evaluation of Green Hydrogen Production via Water Electrolysis for a Sustainable and Clean Energy Society. *Int. J. Hydrogen Energy* **2024**, *52*, 420–441. [CrossRef]
18. Melideo, D.; Ortiz Cebolla, R.; Weidner, E. *Workshop on Lifecycle Analysis of Fuel Cell and H2 Technologies*; Publications Office of the European Union: Luxembourg, 2020.
19. Erbach, G.; Svensson, S. *BRIEFING towards Climate Neutrality*; EU Rules for Renewable Hydrogen; European Parliament Research Service, European Union: Luxembourg, 2023.
20. Ajanovic, A.; Sayer, M.; Haas, R. The Economics and the Environmental Benignity of Different Colors of Hydrogen. *Int. J. Hydrogen Energy* **2022**, *47*, 24136–24154. [CrossRef]
21. Valente, A.; Iribarren, D.; Dufour, J. Harmonised Life-Cycle Global Warming Impact of Renewable Hydrogen. *J. Clean. Prod.* **2017**, *149*, 762–772. [CrossRef]

22. Kolahchian Tabrizi, M.; Famiglietti, J.; Bonalumi, D.; Campanari, S. The Carbon Footprint of Hydrogen Produced with State-of-the-Art Photovoltaic Electricity Using Life-Cycle Assessment Methodology. *Energies* **2023**, *16*, 5190. [CrossRef]
23. Zhang, J.; Wang, Z.; He, Y.; Li, M.; Wang, X.; Wang, B.; Zhu, Y.; Cen, K. Comparison of Onshore/Offshore Wind Power Hydrogen Production through Water Electrolysis by Life Cycle Assessment. *Sustain. Energy Technol. Assess.* **2023**, *60*, 103515. [CrossRef]
24. Krishnan, S.; Corona, B.; Kramer, G.J.; Junginger, M.; Koning, V. Prospective LCA of Alkaline and PEM Electrolyser Systems. *Int. J. Hydrogen Energy* **2024**, *55*, 26–41. [CrossRef]
25. Mio, A.; Barbera, E.; Massi Pavan, A.; Bertucco, A.; Fermeglia, M. Sustainability Analysis of Hydrogen Production Processes. *Int. J. Hydrogen Energy* **2024**, *54*, 540–553. [CrossRef]
26. Hermesmann, M.; Tsiklios, C.; Müller, T.E. The Environmental Impact of Renewable Hydrogen Supply Chains: Local vs. Remote Production and Long-Distance Hydrogen Transport. *Appl. Energy* **2023**, *351*, 121920. [CrossRef]
27. Terlouw, T.; Bauer, C.; McKenna, R.; Mazzotti, M. Large-Scale Hydrogen Production via Water Electrolysis: A Techno-Economic and Environmental Assessment. *Energy Environ. Sci.* **2022**, *15*, 3583–3602. [CrossRef]
28. Henriksen, M.S.; Matthews, H.S.; White, J.; Walsh, L.; Grol, E.; Jamieson, M.; Skone, T.J. Tradeoffs in Life Cycle Water Use and Greenhouse Gas Emissions of Hydrogen Production Pathways. *Int. J. Hydrogen Energy* **2024**, *49*, 1221–1234. [CrossRef]
29. Patel, G.H.; Havukainen, J.; Horttanainen, M.; Soukka, R.; Tuomaala, M. Climate Change Performance of Hydrogen Production Based on Life Cycle Assessment. *Green Chem.* **2024**, *26*, 992–1006. [CrossRef]
30. Zhang, J.; Ling, B.; He, Y.; Zhu, Y.; Wang, Z. Life Cycle Assessment of Three Types of Hydrogen Production Methods Using Solar Energy. *Int. J. Hydrogen Energy* **2022**, *47*, 14158–14168. [CrossRef]
31. Schropp, E.; Campos-Carriedo, F.; Iribarren, D.; Naumann, G.; Bernäcker, C.; Gaderer, M.; Dufour, J. Environmental and Material Criticality Assessment of Hydrogen Production via Anion Exchange Membrane Electrolysis. *Appl. Energy* **2024**, *356*, 122247. [CrossRef]
32. Salah, C.; Cobo, S.; Pérez-Ramírez, J.; Guillén-Gosálbez, G. Environmental Sustainability Assessment of Hydrogen from Waste Polymers. *ACS Sustain. Chem. Eng.* **2023**, *11*, 3238–3247. [CrossRef]
33. Ji, M.; Shi, M.; Wang, J. Life Cycle Assessment of Nuclear Hydrogen Production Processes Based on High Temperature Gas-Cooled Reactor. *Int. J. Hydrogen Energy* **2023**, *48*, 22302–22318. [CrossRef]
34. Weidner, T.; Tulus, V.; Guillén-Gosálbez, G. Environmental Sustainability Assessment of Large-Scale Hydrogen Production Using Prospective Life Cycle Analysis. *Int. J. Hydrogen Energy* **2023**, *48*, 8310–8327. [CrossRef]
35. Chisalita, D.-A.; Petrescu, L.; Galusnyak, S.C.; Cormos, C.-C. Environmental Evaluation of Hydrogen Production Employing Innovative Chemical Looping Technologies—A Romanian Case Study. *Int. J. Hydrogen Energy* **2023**, *48*, 12112–12128. [CrossRef]
36. Williams, J.M.; Bourtsalas, A.C. Assessment of Co-Gasification Methods for Hydrogen Production from Biomass and Plastic Wastes. *Energies* **2023**, *16*, 7548. [CrossRef]
37. Cho, H.H.; Strezov, V.; Evans, T.J. Environmental Impact Assessment of Hydrogen Production via Steam Methane Reforming Based on Emissions Data. *Energy Rep.* **2022**, *8*, 13585–13595. [CrossRef]
38. Ali, S.M.; Alkhatib, I.I.I.; AlHajaj, A.; Vega, L.F. How Sustainable and Profitable Are Large-Scale Hydrogen Production Plants from CH4 and H2S? *J. Clean. Prod.* **2023**, *428*, 139475. [CrossRef]
39. Wijayasekera, S.C.; Hewage, K.; Hettiaratchi, P.; Siddiqui, O.; Razi, F.; Pokhrel, D.; Sadiq, R. Sustainability of Waste-to-Hydrogen Conversion Pathways: A Life Cycle Thinking-Based Assessment. *Energy Convers. Manag.* **2022**, *270*, 116218. [CrossRef]
40. Arfan, M.; Eriksson, O.; Wang, Z.; Soam, S. Life Cycle Assessment and Life Cycle Costing of Hydrogen Production from Biowaste and Biomass in Sweden. *Energy Convers. Manag.* **2023**, *291*, 117262. [CrossRef]
41. Zheng, X.; Wang, J.; Huang, J.; Xu, X.; Tang, J.; Hou, P.; Han, W.; Li, H. Environmental Impact Assessment of a Combined Bioprocess for Hydrogen Production from Food Waste. *Waste Manag.* **2024**, *173*, 152–159. [CrossRef] [PubMed]
42. Sadeghi, S.; Ghandehariun, S. Environmental Impacts of a Standalone Solar Water Splitting System for Sustainable Hydrogen Production: A Life Cycle Assessment. *Int. J. Hydrogen Energy* **2023**, *48*, 19326–19339. [CrossRef]
43. Environmental Performance Indicator. Available online: https://www.environdec.com/resources/indicators (accessed on 16 February 2024).
44. Bauer, C.; Treyer, K.; Antonini, C.; Bergerson, J.; Gazzani, M.; Gencer, E.; Gibbins, J.; Mazzotti, M.; McCoy, S.T.; McKenna, R.; et al. On the Climate Impacts of Blue Hydrogen Production. *Sustain. Energy Fuels* **2022**, *6*, 66–75. [CrossRef]
45. Spath, P.L.; Mann, M.K. *Life Cycle Assessment of Hydrogen Production via Natural Gas Steam Reforming*; National Renewable Energy Laboratory: Golden, CO, USA, 2000.
46. Alhamdani, Y.A.; Hassim, M.H.; Ng, R.T.L.; Hurme, M. The Estimation of Fugitive Gas Emissions from Hydrogen Production by Natural Gas Steam Reforming. *Int. J. Hydrogen Energy* **2017**, *42*, 9342–9351. [CrossRef]
47. Uekert, T.; Wikoff, H.M.; Badgett, A. Electrolyzer and Fuel Cell Recycling for a Circular Hydrogen Economy. *Adv. Sustain. Syst.* **2024**, *8*, 2300449. [CrossRef]

48. Matz, L.; Bensmann, B.; Hanke-Rauschenbach, R.; Minke, C. Resource-Efficient Gigawatt Water Electrolysis in Germany—A Circular Economy Potential Analysis. In *Circular Economy and Sustainability*; Springer: Berlin/Heidelberg, Germany, 2024. [CrossRef]
49. Kiemel, S.; Smolinka, T.; Lehner, F.; Full, J.; Sauer, A.; Miehe, R. Critical Materials for Water Electrolysers at the Example of the Energy Transition in Germany. *Int. J. Energy Res.* **2021**, *45*, 9914–9935. [CrossRef]